

Article

Breakup Dynamics of Droplets in Symmetric Y-Junction Microchannels

Li Lei ¹, Yuting Zhao ^{1,2}, Jun An ^{1,2}, Bo Zhang ^{1,2} and Jingzhi Zhang ^{1,2,3,*} 

¹ School of Energy and Power Engineering, Shandong University, Jinan 250061, China; leili@sdu.edu.cn (L.L.); 201934180@mail.sdu.edu.cn (Y.Z.); 202014435@mail.sdu.edu.cn (J.A.); 202114463@mail.sdu.edu.cn (B.Z.)

² Shandong Engineering Laboratory for High-Efficiency Energy Conservation and Energy Storage Technology & Equipment, School of Energy and Power Engineering, Shandong University, Jinan 250061, China

³ Shenzhen Research Institute of Shandong University, Shenzhen 518057, China

* Correspondence: zhangjz@sdu.edu.cn; Tel.: +86-0531-883-92890

Abstract: The experimental method is used to study the droplet breaking characteristics of an immiscible liquid–liquid two-phase fluid in symmetric Y-junction microchannels. Silicone oil is used as the dispersed phase and distilled water containing 0.5% SDS is used as the continuous phase. Three breakup behaviors were observed: breakup with permanent obstruction, breakup with gaps, and no breakup. Two stages of the change of the neck width of the sub-droplet during the breakup process were discovered: a rapid breakup stage and a thread breakup stage. The effect of the breakup behavior on the flow pattern was investigated and it was found that the breakup behavior of the droplets made the slug flow area smaller; further, a new flow pattern was observed, being droplet flow. The length of the sub-droplet increases with an increase of the volume flow rate of the dispersed phase and the ratio of the volume flow rate of the dispersed phase to the continuous phase, while decreasing with an increase of the volume flow rate and the capillary number of the continuous phase. Based on the influence of the two-phase flow parameters on the length of the sub-droplet, a correlation formula for the length of the sub-droplet with good predictive performance is proposed.

Keywords: breakup dynamics; microchannels; droplet dimensionless length correlation



Citation: Lei, L.; Zhao, Y.; An, J.; Zhang, B.; Zhang, J. Breakup Dynamics of Droplets in Symmetric Y-Junction Microchannels. *Appl. Sci.* **2022**, *12*, 4011. <https://doi.org/10.3390/app12084011>

Academic Editor: Zhifu Zhou

Received: 3 March 2022

Accepted: 12 April 2022

Published: 15 April 2022

Publisher's Note: MDPI stays neutral with regard to jurisdictional claims in published maps and institutional affiliations.



Copyright: © 2022 by the authors. Licensee MDPI, Basel, Switzerland. This article is an open access article distributed under the terms and conditions of the Creative Commons Attribution (CC BY) license (<https://creativecommons.org/licenses/by/4.0/>).

1. Introduction

With the advancement of science and technology, microfluidic technology has also developed rapidly and has received extensive attention in the field of the microchemical industry [1–3]. Microfluidic technology is widely used in bioengineering [4–6], drug screening [7–9], protein crystallization [10], and chemical reactions [11,12] due to its many advantages, such as high safety, high device integration, low consumption of experimental reagents, strong controllability, and process energy saving. In microfluidic technology, the production efficiency can be greatly improved by obtaining two or more sub-droplets at one time by breaking the droplets in the microchannel [13]. Due to the high controllability and repeatability of this breakup method, it has become an important application in microfluidic technology [14–17].

Common microchannel structures used to prepare sub-droplets include T-junction [18,19], Y-junction [20,21], cross-focusing [22], and microchannels with internal obstacles [23]. Among them, these channels can be designed to be symmetrical [24] or asymmetrical [25]. Link et al. [18] investigated droplet breakup within multi-order T-junction microchannels of different lengths and proposed a transition rule for droplet breakup and non-breakup behavior. Jullien et al. [26] conducted an experimental study on droplet breakup within T-junction microchannels at larger capillary numbers and found two breakup mechanisms: microdroplet tunnel breakup and blockage breakup. Rosenfeld et al. [27] studied the breakup process of droplets when a concentrated emulsion flows in a narrow microchannel

with a small pore throat structure. The variation law of droplet divergence with parameters such as flow rate, inlet angle, and droplet size relative to droplet width was studied. Chen et al. [28] used the volume-of-fluid method (VOF) to conduct a 3D simulation of the breakup mechanism of microdroplets in a T-junction microchannel and verified the simulation results through visualization experiments. Through simulations and experimental observations, four breakup modes were discovered and a correlation was proposed to predict the size of the droplet. Cheng et al. [29] used a numerical simulation to study the droplet breakup in asymmetric T-junction microchannels with square cross-sections and different pressure gradient ratios. The critical conditions for the breakup of a droplet into two sub-droplets of different sizes are identified and two main asymmetric breakup mechanisms are proposed: permanently blocked breakup and unstable breakup. Cong et al. [30] used experimental methods to study the breakup behavior of bubbles in an asymmetric Y-junction microchannel, and investigated the effects of two-phase flow rate and physical properties on the distribution of broken bubbles. Three different breakup behaviors were found: asymmetric breakup without a gap, asymmetric breakup with a gap, and no breakup. It can be seen that the research in the existing literature mostly focuses on the T-junction microchannel structure and there is little about the droplet breaking behavior in the symmetrical Y-junction microchannel structure. Furthermore, because of its unique bifurcated structure, Y-junction microchannels are similar to blood vessels in living organisms and have ingenious bionic significance. In order to better control the production of sub-droplets, it is of great significance to study the droplet breaking behavior in symmetric Y-junction microchannels.

In this paper, using silicone oil as the discrete phase and a 0.5 wt % SDS (sodium dodecyl sulfate) aqueous solution as the continuous phase, the droplet breaking behavior in the symmetric Y-junction microchannel was studied by means of visualization experiments. The effect of the breakup behavior on the flow pattern was studied, and the effect of the physical properties of the two-phase fluid on the size of the sub-droplets was investigated. At the same time, a good correlation for predicting the length of sub-droplets is proposed.

2. Experiment System

Figure 1 is a schematic diagram of the experimental system and microchannel used to study the droplet breakup behavior in this paper. The experimental system is divided into four parts: two-phase liquid input system, microchannel reaction system, data acquisition system, and waste liquid collection system. In order to clearly photograph the flow of droplets, an acrylic glass (PMMA) plate with a transmittance of 90% was used as the microfluidic reactor and a 100 W light source was used at the bottom to provide the required brightness. The microchannel is designed as a symmetrical Y-junction entrance and a symmetrical Y-junction bifurcation structure with an angle of 90 degrees and is carved on a PMMA board by a precision engraving machine. The channel consists of two inlets and one outlet, with a square cross-section (400 μm wide \times 400 μm high). Two immiscible liquids from two high-precision syringe pumps (LSP01-1A, Baoding Lange, Baoding, China) were respectively introduced into the two inlets. Silicone oil was used as the dispersed phase, and distilled water containing 0.5 wt % sodium dodecyl sulfate (SDS) was used as the continuous phase. The physical parameters of the fluid are shown in Table 1. The channel outlet leads to a waste bottle, which acts as a waste collection system. A high-speed camera (Photron Nova S6, Tokyo, Japan) was placed right above the microfluidic reactor, saving 2000 frames per second, and the captured data was transmitted to a computer in real time for data acquisition and recording.

For ease of discussion and understanding, a schematic diagram of the relevant parameters of the droplet breakup process in this work is given in Figure 2. Among them, W is the main channel width, W_m is the neck width during the droplet breakup process, and L_d is the sub-droplet length after the droplet breakup.

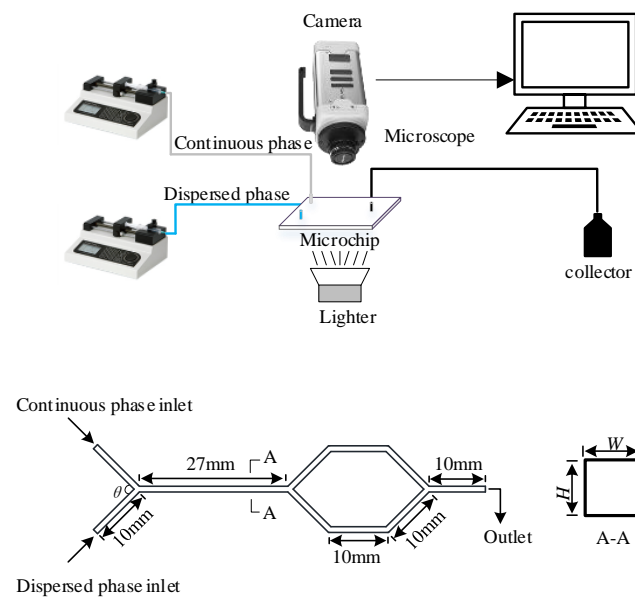


Figure 1. Schematic diagram of the experimental system and microchannel.

Table 1. Fluid properties.

Fluid System		$\mu/(\text{Pa}\cdot\text{s})$	$\rho/(\text{kg}\cdot\text{m}^{-3})$	$\gamma/(\text{N}\cdot\text{m}^{-1})$
Continuous phase	0.5 wt % SDS	0.00135	971.53	–
Discrete phase	Silicone oil	0.01	901.4	0.0118

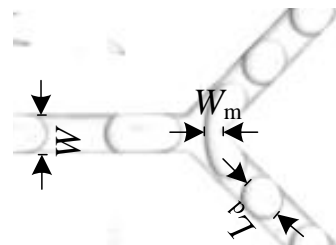


Figure 2. Definition of parameters related to droplet breakup.

3. Experimental Results and Discussion

3.1. Droplet Breakup Process

Figure 3 shows the droplet breakup process in a symmetric Y-junction microchannel. The operating flow range of this paper is $q_d = 2\text{--}18\text{ mL/h}$, $q_c = 2\text{--}22\text{ mL/h}$, and it is found that the behavior of the droplet at the symmetric Y-junction bifurcation is divided into two types: breakup and no breakup. In the breakup behavior, it is divided into two breakup modes: breakup with permanent obstruction and breakup with gaps. No matter what kind of breakup mode, it can be divided into three stages: entry stage, deformation stage, and breakup stage. The droplet breakup behavior inside the microreactor was captured using a high-speed camera and the frame rate was set to 2000 fps. The time interval of each picture can be calculated according to the frame rate. By calculating the product of the number of pictures and the interval time of each picture, the instantaneous time represented by any picture can be calculated. In all processes, the droplet head just reached the bifurcation as the start time of the droplet breakup process, and the moment when the droplet breaks as the two sub-droplets as the end time of the droplet breakup process. Taking the breakup with a permanent obstruction as an example, from 0–13.7 ms, the head of the droplet completely fills the Y-junction bifurcation and this moment is the sign of the end of the entry stage. From 13.7–43.7 ms, after the end of the entry stage, the droplet gradually expanded and deformed, eventually filling the two branch channels with the

passage of time, thus forming the neck of the droplet. The appearance of the droplet neck is a sign of the end of the deformation phase. From 43.7 to 52.7 ms, the droplet neck gradually becomes thinner until the neck width is 0, at which time the droplet breaks into two sub-droplets. The sign to distinguish gapless breakup from gapped breakup is whether the droplet separates from the microchannel wall during the process of entering the branch channel until breakup. As shown in Figure 3a, if the droplets always contact the wall of the microchannel, there is breakup with permanent obstruction. As shown in Figure 3b, after 28 ms, there is a gap between the droplet and the wall of the microchannel, which is a breakup with gaps. As shown in Figure 3c, the droplet selectively entered the unilateral branch channel and did not break into two sub-droplets, which is the case of no breakup.

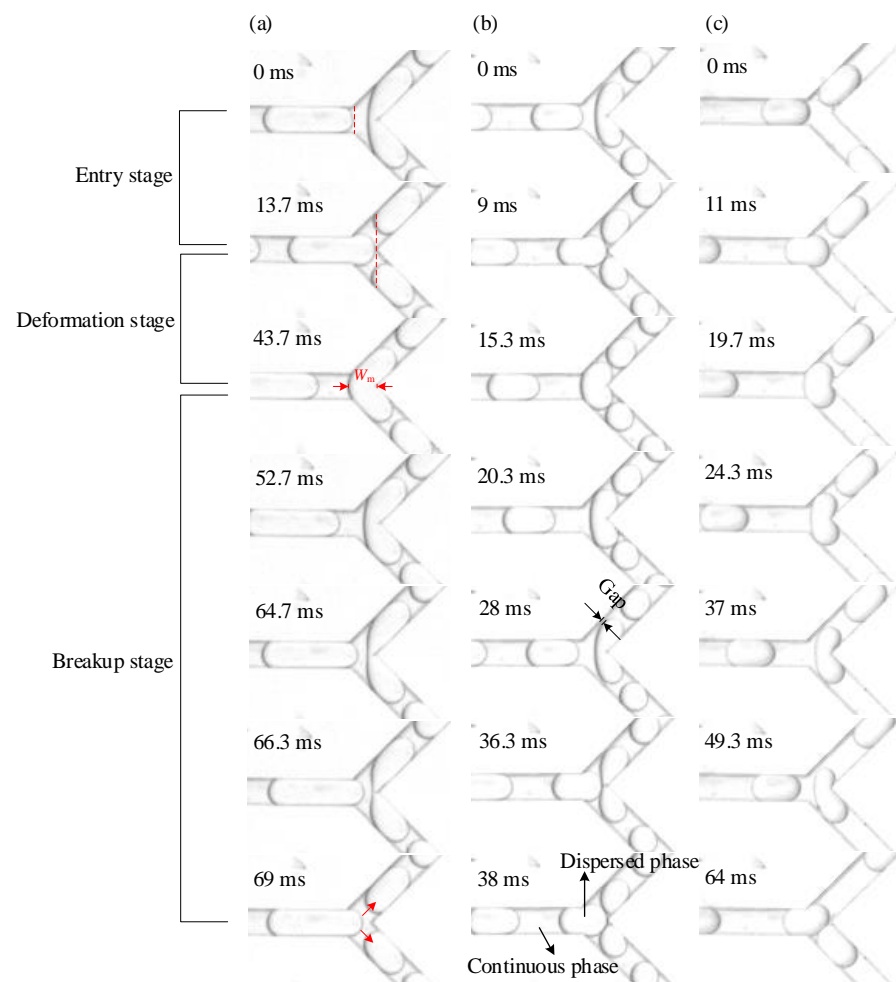


Figure 3. Breaking process of liquid drop in symmetric Y-junction microchannel: (a) breakup with permanent obstruction; (b) breakup with gaps; (c) no breakup.

Figure 4 shows the variation of the droplet neck width during the breakup stage. Among them, t_p refers to the total time of the droplet breakup process, that is, the droplet breakup period. It is defined as the time interval from the droplet head just reaching the bifurcation to the droplet breaking into sub-droplets, with t being a certain moment in the breakup process. It is defined as the time interval from the droplet head just reaching the bifurcation to the droplet breaking into sub-droplets.

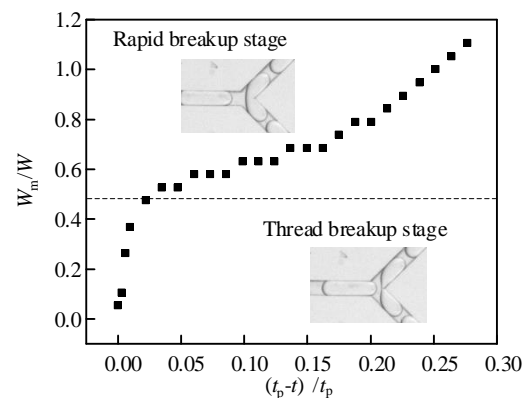


Figure 4. Changes in the width of the droplet neck during the breakup stage.

It can be clearly seen that there are two distinct stages in the rate of change of the dimensionless neck width W_m/W with the dimensionless remaining time throughout the breakup process. In the first stage, W_m/W decreased with an increase of time, and the decreasing rate gradually became slower, which was defined as the rapid breakup stage. In the second stage, W_m/W also decreased with the increase of time, but the difference was that the rate of decrease was much greater than that of the first stage, and it gradually increased with the increase of time. This is due to the fact that the droplet breakup is mainly affected by the differential pressure force and the shear force from the continuous phase. In the rapid breakup stage, the area of the two-phase interface in contact with the continuous phase is small, so it is mainly affected by the differential pressure force, so the breakup rate is small. As the droplet grows into the branch channel, the contact area between the two-phase interface and the continuous phase is relatively large when the neck reaches the state of filament adhesion. Therefore, the droplets are subjected to a relatively large shear force from the continuous phase and break up faster [5]. Since the transition in the rate of change of W_m/W begins with the appearance of filamentous adhesions at the neck of the droplet, the second stage is defined as thread breakup stage. The rapid breakup stage occupies a very long time in the whole breakup process, while the filament breakup phase occupies only a small part.

3.2. Flow Pattern

Figure 5 shows the flow pattern according to the breakup mode in the symmetrical Y-junction microchannel. Take the dispersed phase flow q_d as the abscissa and the continuous phase flow q_c as the ordinate. Clearly, the way the droplets break up changes with the two-phase flow. When q_d is constant, with an increase of q_c , the breaking method of the droplet changes from breaking to not breaking. This is due to the fact that the length of the droplet becomes smaller as the q_c increases and it is easier to choose to enter one of the branch channels such that breakup does not occur. Clearly, when the two-phase flow rates are relatively small, the droplets are more prone to no-breakup behavior. This is because as the capillary number of the two phases is small, the shear force on the droplet is small, which is not enough to overcome the effect of surface tension and the droplet is not easy to break. When the q_d is relatively small, the droplet breakup mode is only gapless breakup and no breakup. When the q_d is relatively large, the droplet will experience breakup with permanent obstruction, breakup with gaps and no breakup with the increase of q_c .

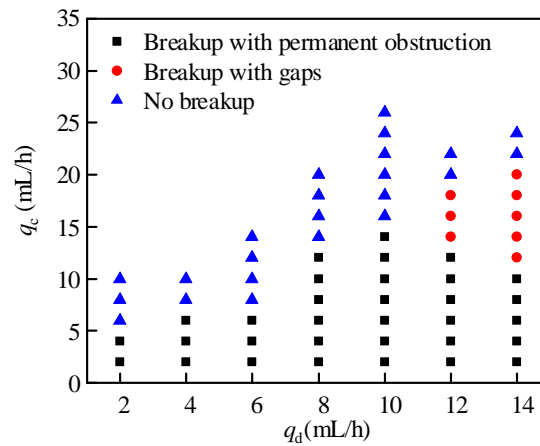


Figure 5. Flow pattern diagram based on breakup mode.

In the study of two-phase flow, the flow pattern is the basis of all problems. Different application backgrounds have different requirements for flow patterns, so it is of far-reaching significance to study the effect of breakup on flow patterns. It is worth noting that the division of the flow pattern at this time is based on the length of the droplet. In general, the microchannel cross-sectional size has an effect on the droplet length. In order to reduce the influence of different microchannel cross-sectional dimensions on the droplet length, a dimensionless droplet length L_d/W is defined, where L_d refers to the droplet length and W refers to the channel width. Parallel flow refers to the flow pattern in which the dispersed phase does not break, slug flow refers to droplets with dimensionless length $L_d/W > 1.5$, and droplet flow refers to droplets with $L_d/W < 1.5$. As shown in Figure 6a, when q_d is relatively large and q_c is relatively small, parallel flow is likely to be generated. This is because the dispersed phase has a large inertial force when the dispersed phase flow is large. When the inertial force of the dispersed phase plays a dominant role in the two-phase flow, the dispersed phase can maintain continuous flow in the microchannel without being sheared by the continuous phase. At this time, the dispersed phase flows continuously in the main channel, and the continuous phase flows around the dispersed phase near the wall of the microchannel. In the two-phase operating flow range in this paper, the vast majority of flow patterns in the microchannels without breakup behavior are slug flow. As shown in Figure 6b, parallel flow cannot be observed in the microchannel after the droplet is broken, and a new flow pattern: droplet flow appears. In addition, the area occupied by the slug flow in the flow pattern becomes smaller. Clearly, the droplet breakup behavior has a significant effect on the flow pattern.

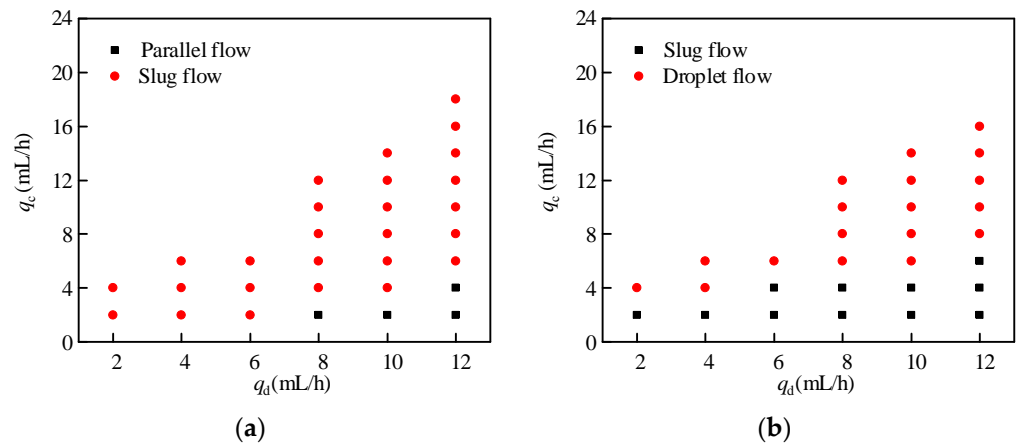


Figure 6. Effect of breakup behavior on droplet flow pattern: (a) flow pattern before the droplet breakup; (b) flow pattern after the droplet breakup.

3.3. Influence of Two-Phase Fluid Parameters on Sub-Droplet Length

Figure 6 shows the effect of the two-phase flow parameters on the sub-droplet length. The definition formulas of the continuous phase capillary number Ca_c and the two-phase flow ratio q are as follows. W represents the width of the microchannel and H represents the depth of the microchannel.

$$Ca_c = \frac{\left(\frac{q_c}{W \times H}\right) \times \mu_c}{\sigma}, \quad (1)$$

$$q = \frac{q_d}{q_c} \quad (2)$$

Figure 7a,b shows the effect of the two-phase flow on the sub-droplet length. The sub-droplet length decreases with the increase of the continuous phase flow rate and increases with the increase of the dispersed phase flow rate. This is due to the fact that the inertial force of the dispersed phase increases with the flow rate and the head of the dispersed phase is more likely to move forward, thereby forming longer droplets. At a certain speed, as the flow rate of the continuous phase increases, the shear force between the two phases increases. As the shearing effect of the continuous phase is greater, the droplets are more easily broken up at higher continuous phase flow rates. The change in droplet length is inseparable from the interaction of the two phases. The size of the broken sub-droplets increases with the size of the generated droplets. Conversely, smaller droplets correspond to smaller sub-droplets. Figure 7c,d shows the influence of the dimensionless length L_d/W of the sub-droplet with the continuous phase capillary number Ca_c and the two-phase flow ratio q on the length of the sub-droplet. The dimensionless length of sub-droplets (L_d/W) increases with increasing q and decreases with increasing capillary number (Ca_c) of the continuous phase. This is because when the droplet q is relatively large, the q_d is relatively large and the q_c is relatively small; as such, the inertial force of the dispersed phase is relatively large and the shearing effect of the continuous phase is relatively small, making it is easier to generate longer droplets. Ca_c is proportional to the ratio of viscous force and surface tension. The larger the Ca_c , the larger the viscous force relative to the surface tension. The length of the droplets becomes shorter as the shearing action of the continuous relative dispersed phase increases. Likewise, larger droplets correspond to larger sub-droplets.

3.4. Droplet Length Correlation

As mentioned earlier, the dimensionless length L_d/W of the sub-droplets is positively correlated with q and negatively correlated with Ca_c . Therefore, L_d/W can be written as a function of q and Ca_c , where only the coefficients change. It can be seen from the correlation that the effect of the two-phase flow rate ratio q on the droplet length is positively correlated, while the effect of the continuous phase capillary number Ca_c on the droplet length is negatively correlated. The law of this correlation is consistent with the conclusion in Section 3.3. According to the experimental data, the length correlation of the sub-droplets generated by the breakup behavior in the symmetric Y-junction microchannel is fit as shown in Formula (3):

$$L_d/W = 0.593q^{0.385}Ca_c^{-0.11} \quad (3)$$

Figure 8 shows the error comparison between the experimental value of the sub-droplet length in the microchannel and the predicted value of the correlation. Obviously, the error range between the predicted value of the correlation and the experimental value is within $\pm 20\%$. The predictive performance of length correlations was quantitatively described using mean absolute deviation (MAD) and mean relative deviation (MRD). MAD and MRD are shown in Formulas (4) and (5), respectively. The MAD was 6.5% and the

MRD was -1% . In summary, it shows that the droplet length correlation proposed in this paper can better predict the experimental results.

$$MAD = \frac{1}{N} \sum_{i=1}^N \frac{|U_{pre} - U_{exp}|}{U_{exp}} \times 100\% \quad (4)$$

$$MRD = \frac{1}{N} \sum_{i=1}^N \frac{U_{pre} - U_{exp}}{U_{exp}} \times 100\% \quad (5)$$

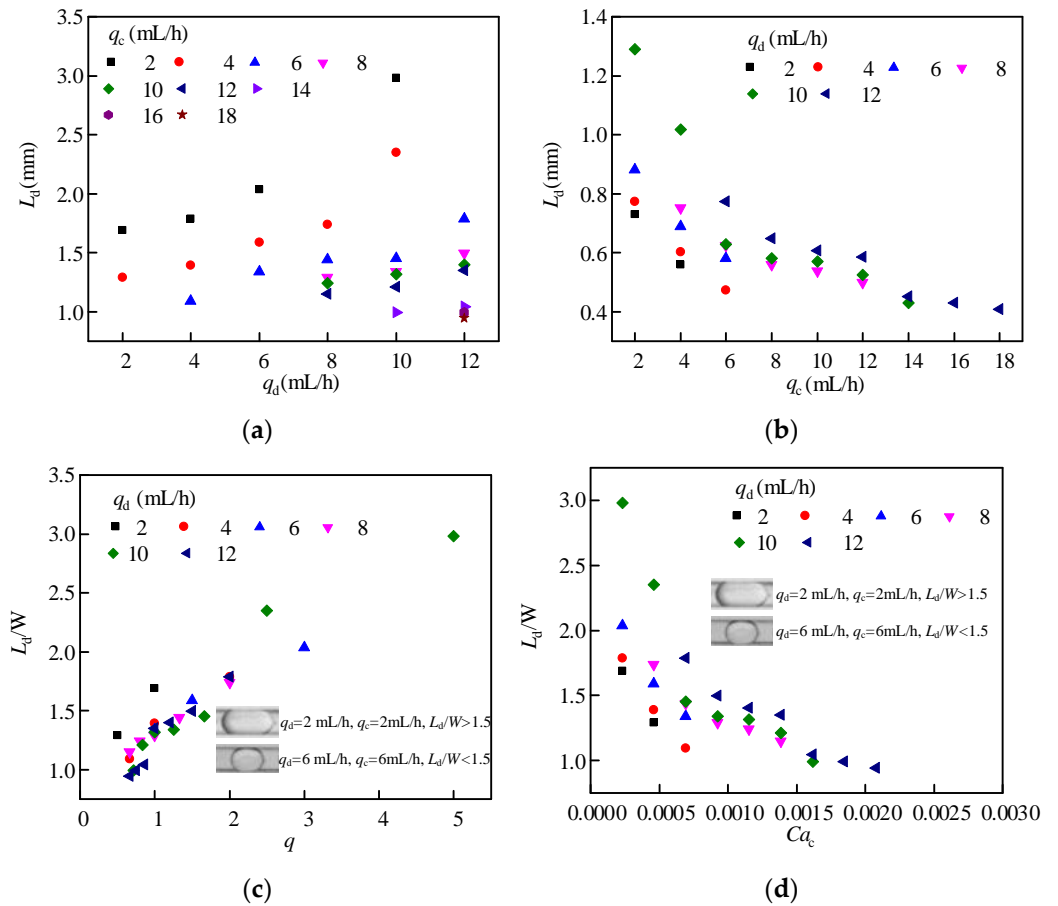


Figure 7. Influence of two-phase fluid parameters on the length of sub-droplets: (a) q_d , (b) q_c , (c) q , and (d) Ca_c .

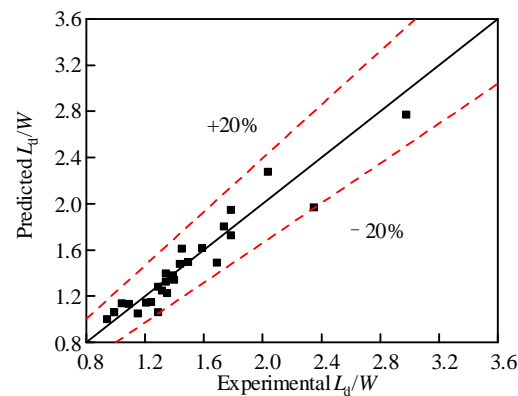


Figure 8. Comparison of the experimental value of the sub-droplet length and the predicted value of the correlation formula.

4. Conclusions

In this paper, the characteristics of droplet breakup in symmetrical Y-junction microchannels were studied under the flow rate range of $q_d = 2\sim 18$ mL/h for the discrete phase and the flow rate range of $q_c = 2\sim 22$ mL/h for the continuous phase. Among them, the liquid–liquid two-phase uses silicone oil as the dispersed phase and distilled water with 0.5% SDS as the continuous phase. The main conclusions are as follows:

- (1) At the two-phase flow ranges covered in this paper, three modes of breakup were observed: breakup with permanent obstruction, breakup with gaps, and no breakup. Three stages in the droplet breakup process were found: the entry stage, the deformation stage, and the breakup stage. The change of neck width during droplet breakup has two stages: rapid breakup stage and thread breakup stage;
- (2) The breakup behavior of droplets has a significant impact on the flow pattern. Before breakup, most flow patterns are slug flow. After breakup, no parallel flow can be observed in the microchannel and a new flow pattern, droplet flow, appears. Moreover, the area occupied by the slug flow in the flow pattern becomes smaller after breakup;
- (3) Two-phase flow parameters affect the length of the sub-droplets after breakup. The droplet length has a positive correlation with the discrete-phase flow q_d and a negative correlation with the continuous-phase flow q_c ; the dimensionless droplet length L_d/W has a positive correlation with the two-phase flow ratio q and a negative correlation with the capillary number. According to this rule, the correlation formula of sub-droplet length is proposed and the prediction effect is good.

Author Contributions: Conceptualization, L.L. and J.Z.; methodology, Y.Z.; validation, L.L., J.A. and Y.Z.; formal analysis, B.Z.; investigation, L.L. and Y.Z.; resources, J.Z.; data curation, Y.Z.; writing—original draft preparation, Y.Z. and L.L.; writing—review and editing, L.L.; supervision, L.L.; project administration, L.L. and J.Z.; funding acquisition, J.Z. All authors have read and agreed to the published version of the manuscript.

Funding: This research was funded by the Guangdong Basic and Applied Basic Research Foundation (2019A151511116), Shandong Province Natural Science Foundation (No. ZR2021ME080), Shandong Provincial Postdoctoral Innovation Project (No. 201902002), Foundation of Shandong University for Young Scholar's Future Plans, and Double First-Class Foundation for the Talents of Shandong University (31380089963090).

Institutional Review Board Statement: Not applicable.

Informed Consent Statement: Not applicable.

Data Availability Statement: Not applicable.

Acknowledgments: We thank the Guangdong Basic and Applied Basic Research Foundation, the Shandong Province Natural Science Foundation, and Shandong University for the fundings.

Conflicts of Interest: The authors declare no conflict of interest.

References

1. Garstecki, P.; Fuerstman, M.J. Formation of droplets and bubbles in a microfluidic T-junction—scaling and mechanism of break-up. *Lab Chip* **2006**, *6*, 437–446. [[CrossRef](#)]
2. Lei, L.; Zhao, Y.T. Experimental Studies of Droplet Formation Process and Length for Liquid-Liquid Two-Phase Flows in a Microchannel. *Energies* **2021**, *14*, 1341. [[CrossRef](#)]
3. Zhang, J.; Li, W. Investigation of hydrodynamic and heat transfer characteristics of gas-liquid Taylor flow in vertical capillaries. *Int. Commun. Heat Mass Transf.* **2016**, *74*, 1–10. [[CrossRef](#)]
4. Abkarian, M.; Faivre, M. Swinging of red blood cells under shear flow. *Phys. Rev. Lett.* **2007**, *98*, 188302. [[CrossRef](#)]
5. Zhang, Q.; Liu, H. Hydrodynamics and mass transfer characteristics of liquid-liquid slug flow in microchannels: The effects of temperature, fluid properties and channel size. *Chem. Eng. J.* **2019**, *358*, 794–805. [[CrossRef](#)]
6. Zhao, S.; Wang, W. Mixing performance and drug nano-particle preparation inside slugs in a gas-liquid microchannel reactor. *Chem. Eng. Sci.* **2013**, *100*, 456–463. [[CrossRef](#)]
7. Guo, M.T.; Rotem, A. Droplet microfluidics for high-throughput biological assays. *Lab Chip* **2012**, *12*, 2146–2155. [[CrossRef](#)]
8. Bhise, N.S.; Ribas, J. Organ-on-a-chip platforms for studying drug delivery systems. *J. Control. Release* **2014**, *190*, 82–93. [[CrossRef](#)]

9. Ozcelikkale, A.; Moon, H.R. In Vitro microfluidic models of tumor microenvironment to screen transport of drugs and nanoparticles. *Wiley Interdiscip. Rev.-Nanomed. Nanobiotechnol.* **2017**, *9*, e1460. [[CrossRef](#)] [[PubMed](#)]
10. Zheng, B.; Gerds, C.J. Using nanoliter plugs in microfluidics to facilitate and understand protein crystallization. *Curr. Opin. Struct. Biol.* **2005**, *15*, 548–555. [[CrossRef](#)] [[PubMed](#)]
11. Shum, H.C.; Bandyopadhyay, A. Double Emulsion Droplets as Microreactors for Synthesis of Mesoporous Hydroxyapatite. *Chem. Mater.* **2009**, *21*, 5548–5555. [[CrossRef](#)]
12. Chen, H.; Zhao, Y. Reactions in double emulsions by flow-controlled coalescence of encapsulated drops. *Lab Chip* **2011**, *11*, 2312–2315. [[CrossRef](#)] [[PubMed](#)]
13. Fu, T.T.; Xu, Z.Y. Progress in breakup dynamics of droplets and bubbles in microchannels. *CIESC J.* **2018**, *69*, 4566–4576.
14. Fu, T.; Wu, Y. Droplet formation and breakup dynamics in microfluidic flow-focusing devices: From dripping to jetting. *Chem. Eng. Sci.* **2012**, *84*, 207–217. [[CrossRef](#)]
15. Bedram, A.; Moosavi, A. Droplet breakup in an asymmetric microfluidic T junction. *Eur. Phys. J. E* **2011**, *34*, 1–8. [[CrossRef](#)]
16. Liu, X.; Zhang, C. Bubble breakup in a microfluidic T-junction. *Sci. Bull.* **2016**, *61*, 811–824. [[CrossRef](#)]
17. Gao, W.; Yu, C. Droplets breakup via a splitting microchannel. *Chin. Phys. B* **2020**, *29*, 054702. [[CrossRef](#)]
18. Link, D.R.; Anna, S.L. Geometrically mediated breakup of drops in microfluidic devices. *Phys. Rev. Lett.* **2004**, *92*, 054503. [[CrossRef](#)]
19. De Menech, M. Modeling of droplet breakup in a microfluidic T-shaped junction with a phase-field model. *Phys. Rev. E* **2006**, *73*, 031505. [[CrossRef](#)]
20. Yamada, M.; Doi, S. Hydrodynamic control of droplet division in bifurcating microchannel and its application to particle synthesis. *J. Colloid Interface Sci.* **2008**, *321*, 401–407. [[CrossRef](#)]
21. Zheng, M.; Ma, Y. Effects of topological changes in microchannel geometries on the asymmetric breakup of a droplet. *Microfluid. Nanofluid.* **2016**, *20*, 107. [[CrossRef](#)]
22. Cubaud, T. Deformation and breakup of high-viscosity droplets with symmetric microfluidic cross flows. *Phys. Rev. E* **2009**, *80*, 026307. [[CrossRef](#)] [[PubMed](#)]
23. Ma, Y.; Zheng, M. Effects of obstacle lengths on the asymmetric breakup of a droplet in a straight microchannel. *Chem. Eng. Sci.* **2018**, *179*, 104–114. [[CrossRef](#)]
24. Okushima, S.; Nisisako, T. Controlled production of monodisperse double emulsions by two-step droplet breakup in microfluidic devices. *Langmuir* **2004**, *20*, 9905–9908. [[CrossRef](#)] [[PubMed](#)]
25. Ma, P.C.; Zhu, C.Y. Dynamics of droplet breakup with permanent tunnel in asymmetric microfluidic T-junction. *CIESC J.* **2018**, *69*, 4633–4639.
26. Jullien, M.C.; Tsang Mui Ching, M.J. Droplet breakup in microfluidic T-junctions at small capillary numbers. *Phys. Fluids* **2009**, *21*, 072001. [[CrossRef](#)]
27. Rosenfeld, L.; Fan, L. Break-up of droplets in a concentrated emulsion flowing through a narrow constriction. *Soft Matter* **2014**, *10*, 421–430. [[CrossRef](#)]
28. Chen, B.; Li, G. 3D numerical simulation of droplet passive breakup in a micro-channel T-junction using the Volume-Of-Fluid method. *Appl. Therm. Eng.* **2015**, *88*, 94–101. [[CrossRef](#)]
29. Cheng, W.L.; Sadr, R. Prediction of Microdroplet Breakup Regime in Asymmetric T-Junction Microchannels. *Biomed. Microdevices* **2018**, *20*, 72. [[CrossRef](#)]
30. Cong, Z.X.; Zhu, C.Y. Bubble breakup and distribution in asymmetric Y-bifurcating microchannels. *CIESC J.* **2014**, *65*, 93–99.